



## Nanocrystalline Al-doped ZnO thin films with enhanced CO gas sensing characteristics

Raghu V. Vidap<sup>1</sup>, Kisan V. Zipare<sup>2</sup>, Sushilkumar S. Bandgar<sup>3</sup>,  
Guruling S. Shahane<sup>3</sup>

<sup>1</sup>Modern College of Arts, Science and Commerce, Pune, India.

<sup>2</sup>C.B.Khedgi's B. Sci., R. V. Comm. and R. J. Arts College,  
Akkalkot, India.

<sup>3</sup>DBF Dayanand College of Arts and Science, Solapur, India.



### ABSTRACT

A sol-gel spin coating method is used to synthesize Al-doped ZnO thin films. The XRD studies show synthesis of phase pure ZnO thin films with hexagonal wurtzite structure. The lattice parameters are  $a=3.2568\text{\AA}$  and  $c=5.2108\text{\AA}$  and decreases with Al-doping concentration. The doping also enhances the preferential growth along (002) direction. SEM studies show that with Al-doping the growth of the films takes place with porous structure embedded with nanogranules overgrown on the folded structure. This indicates that Al-doping has an influence on the surface morphology of the films. Transmission electron microscopy was used to confirm the nanocrystalline nature of the samples. The lattice fringes of the core, as observed from the HRTEM images, also confirms the single crystalline nature with lattice spacing about 0.26nm which corresponds to (002) lattice plane. Gas sensing characteristics showed that ZnO films are sensitive as well as fast responding to CO gas at 250°C. The sensor response increases with Al-doping concentration up to 1wt% and saturates afterwards. A high sensitivity for CO gas indicates that the ZnO films are selective for this gas. The enhanced sensor response is due to small crystallite size, modifications in the electron Debye length and modifying the gas-surface interactions.

**KEYWORDS:** ZnO: Al thin films; sol gel process; structural characterization; CO gas sensor.

### 1. Introduction

Gas sensors based on metal oxide sensitive layers are playing an important role in the detection of toxic pollutants and inflammable gases. One-dimensional and quasi-one-dimensional nanostructures have fascinated both intensive and extensive research, owing to their unique advantages arising from low dimensionality and use in novel nanodevices. The high surface to volume ratio of these low dimensional nanostructures is particularly useful for increasing their electrical properties due to the extremely sensitive surface chemical reactions. Zinc oxide with a wide band gap ( $E_g = 3.37\text{ eV}$ ) is one of the most important and extensively used metal oxide semiconductor materials for gas sensors [1-3]. Since the gas sensing properties are strongly dependent on the surface of the materials exposed to gases, the sensor based on thin film nanostructures of semiconducting metal oxide materials are expected to exhibit better sensitive properties than bulk. Microstructure control of the sensing materials, especially the grain size and porosity, hence become fundamental for the enhancement of gas-sensing performance. Various techniques have been used to deposit pure and doped ZnO thin films on different substrates. These include spray pyrolysis, chemical bath deposition, hydrothermal, RF sputtering, SILAR, CVD and sol-gel [4-12]. Among these, the sol-gel technique has several advantages, such as deposition of high purity, homogeneous, cheaper, large-area films at relatively low temperatures.

The major drawback of undoped ZnO gas sensor material is its low sensitivity and selectivity. The sensing response of these low-dimensional nanostructures can also be improved by adding predetermined amount of impurities and active species on their surface. Thus the study of effect of dopants on the properties of ZnO based nanostructures is very important. Compared to undoped semiconductors, doped materials offer the possibility of using the dopant to tune their electronic properties thereby altering their gas sensing properties. Recent research reveals that ZnO films doped with Mn, Ni, Cu, Au, Sn, Pt, Co, Sb, etc. show modifications in gas sensing properties [9, 13-16]. The implantation of the dopants increased the sensitivity and the selectivity towards many gases. However, there are scarcely any reports on the effect of aluminum doping on the structure, morphology and gas sensing properties of ZnO films prepared by the sol-gel spin coating technique. Among the various gases, CO is toxic gas, acting by reaction with hemoglobin and reducing its capacity for oxygen transport in the blood and thus it is very essential to monitor the CO gas concentration in the environment. In this paper, we report on the structural, morphological and CO gas sensing properties of Al-doped ZnO thin films synthesized by sol-gel spin coating technique.

## 2. EXPERIMENTAL DETAILS

Pure and aluminum doped ZnO thin films were deposited onto glass substrates by sol-gel spin coating method [12]. For deposition AR grade zinc acetate dehydrate, aluminum sulphate, 2-methoxyethanol and monoethanolamine (MEA) were used as the starting materials. The sol was prepared by dissolution of zinc acetate dehydrate in 2-methoxyethanol and monoethanolamine (MEA).  $\text{Al}_2(\text{SO}_4)_3 \cdot 16\text{H}_2\text{O}$  was dissolved in water and added to the host solution in the appropriate proportion. The prepared solution was stirred at 80°C for 20 minutes to get clear and homogeneous solution. The film was then deposited onto glass substrates by using spin coating unit (MILMAN-XT56), which was rotated at 3000 rpm for 2 minutes. After depositing by spin coating, the film was dried at 200°C for 10 minutes in a furnace to evaporate the solvent and remove organic residuals. The film was then annealed in air at 400°C for 4 h.

The thin films were then characterized through X-ray diffraction technique for its structural analysis. A Philips PW-3710 X-ray diffractometer with  $\text{CuK}\alpha$  radiation ( $\lambda = 1.54056 \text{ \AA}$ ) was used for this purpose. The range of  $2\theta$  angle was from 20° to 80°. The surface morphology of the thin films was observed on SEM (JEOL JSM 6360) operating at 20 kV. The shape and microstructure of the samples were analyzed by using transmission electron microscope (JEM-2100 JEOL). For gas sensing characterization, a custom developed gas sensing measurement setup was used. The sensor element was kept in an air tight chamber of volume 250 ml. Two silver electrodes, separated by 1 mm, were deposited on ZnO film. A predefined concentration of gas was introduced in this chamber by a syringe. The operating temperature of the sensor was varied from 100-400°C. The response of the sensor was measured using ARM processor based data acquisition system designed and developed in the laboratory. The sensor was tested for various gases like  $\text{H}_2\text{S}$ ,  $\text{NH}_3$ , CO,  $\text{H}_2$  and  $\text{CH}_4$ . The stabilization of the ZnO film resistance in ambient air prior to exposure of gas is important because it ensures stable zero level for gas sensing applications. Hence before exposing the gas over the ZnO film, it was allowed to become stable for electrical resistance.

## 3. RESULTS AND DISCUSSION

The deposited films are thin, uniform and strongly adhering to the glass substrate. The X-ray diffractograms of pure and doped ZnO thin films are shown in Fig. 1.

The patterns were analyzed to get the information about crystal structure, lattice parameters and grain size. The d-values and intensities of the observed diffraction peaks match with the single crystalline form of the hexagonal ZnO (JCPD card no. 036-1451) indicating that synthesized sample is zinc oxide with hexagonal wurtzite structure. No separate aluminum phase is detected, however, the peak positions shifts towards higher  $2\theta$  values (Fig. 1 inset), which supports that Al ions are substituted at Zn sites entirely in the lattice of ZnO crystal. It is observed that for pure ZnO the strongest reflection

is (101) plane. With Al-doping the intensity of (002) reflection gradually increases and becomes the strongest

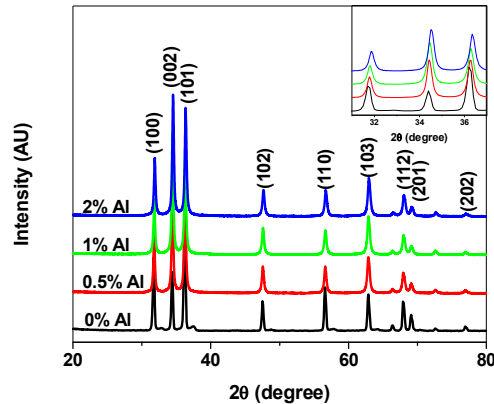


**Fig. 1 X-ray diffractograms of Al-doped ZnO thin films**

reflection. This suggests Al-doping enhances the preferential growth along (002) direction. Lattice parameters were then calculated from the d values and the values are listed in Table 1.

**Table 1: Structural analysis of ZnO: Al thin films**

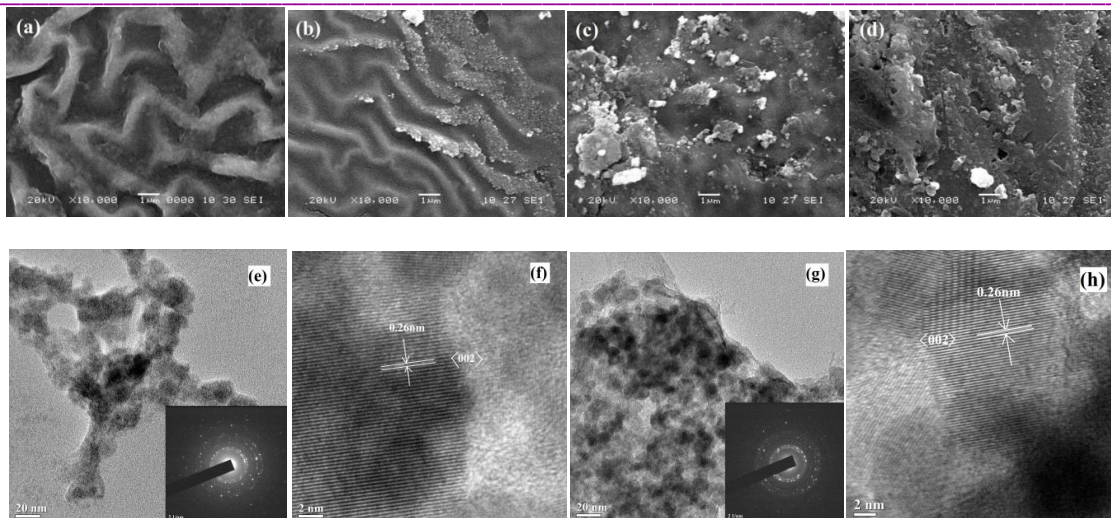
Al-doping Concentration (Wt%)	Lattice Parameters		Grain Size (nm)
	a (Å)	c (Å)	
0	3.2568	5.2108	58.8
0.5	3.2503	5.2079	60.9
1	3.2483	5.2020	56.8
2	3.2413	5.1947	58.8

The lattice parameters decrease with increase in Al-doping concentration. As the covalent radius of Al (0.118 nm) is smaller than that of Zn (0.131 nm), incorporation of Al<sup>3+</sup> at the interstitial positions of ZnO sub-lattice leads to decrease in lattice parameter which is indicated by the gradual shift in the peak positions towards higher 2θ values [17]. The average crystallite size was determined by using the Scherer's relation:

$$D = 0.89 \lambda / \beta \cos \theta \quad (1)$$

where,  $D$  is the crystallite size,  $\lambda$  is wavelength of X-ray,  $\beta$  is full width at half maximum (FWHM) measured in radians and  $\theta$  is the Bragg angle. The values of average crystallite are listed in Table 1. It is observed that the average crystallite size is in the range of 56-61 nm for all the samples.

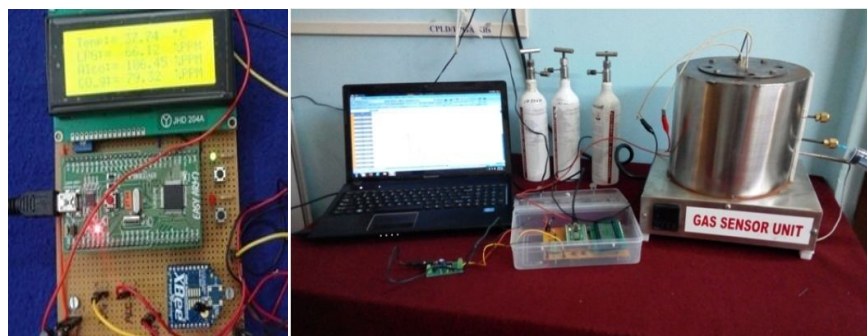
The morphology and structure of the samples was observed by using scanning electron microscope (SEM) and transmission electron microscope (TEM).



**Fig. 2 Surface morphology of Al-doped ZnO thin films:**  
**SEM images: (a) 0% Al, (b) 0.5% Al, (c) 1% Al and (d) 2% Al.**  
**TEM, SAED, HRTEM images: (e, f) 0% Al and (g, h) 1% Al.**

Fig. 2(a-d) shows the SEM images of pure and Al-doped ZnO thin films. For pure ZnO it is seen that the growth of the film takes place with folded structure increasing the open surface area of the film. With Al-doping the growth of the films takes place with porous structure embedded with nanogranules overgrown on the folded structure. This indicates that Al-doping has an influence on the surface morphology of the films. The TEM images, the selected area electron diffraction (SAED) patterns and the high resolution TEM (HRTEM) images of ZnO: Al thin films for two typical compositions are shown in Fig. 2(e-h). The sample contains nanoparticles of nearly spherical in shape with narrow size distribution. The SAED patterns (Inset figures) provide the d-spacing consistent with those obtained from XRD studies. The lattice fringes of the core, as observed from the HRTEM images, also confirm the single crystalline nature with lattice spacing about 0.26nm which corresponds to (002) plane. These observations imply that high quality uniform ZnO thin films are obtained with this method.

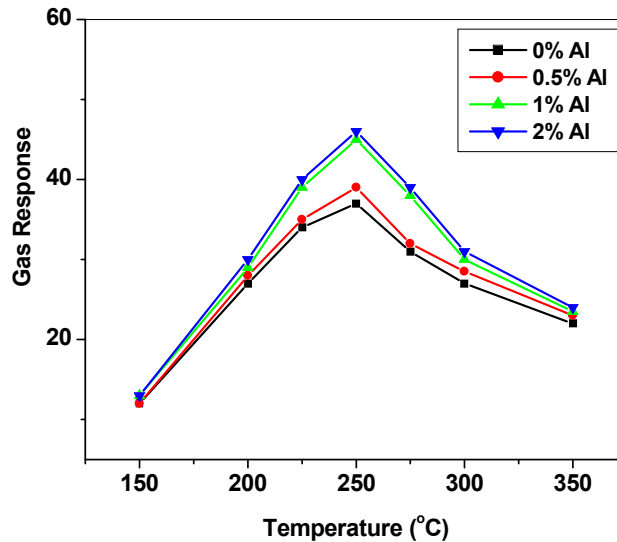
The gas sensing properties of ZnO thin films were studied in terms of its sensitivity, selectivity, temperature dependence and speed of response. The experimental arrangement for the characterization of gas sensor element is shown in Fig. 3.



**Fig. 3 Experimental setup for characterization of thin film gas sensor**

The details about the development of ARM microcontroller based data acquisition system are reported elsewhere [18]. In general, the metal oxide thin film sensors show sensitivity towards many

oxidizing or reducing gases depending on the surface morphology, film porosity, operating temperature and presence of additives. As our main intension is to detect the toxic CO gas, the gas sensing properties of Al-doped ZnO films were first carried out for the CO gas. It is observed that resistance of the ZnO film decreases with the CO gas concentration. Since the response of the sensor to a target gas depends on the temperature of the sensor element, it is essential to optimize the operating temperature of the ZnO sensor to give maximum sensitivity and selectivity towards CO gas. For this the sensor element was exposed to 100 ppm concentration of CO gas and its response was recorded in 100-400°C temperature range.



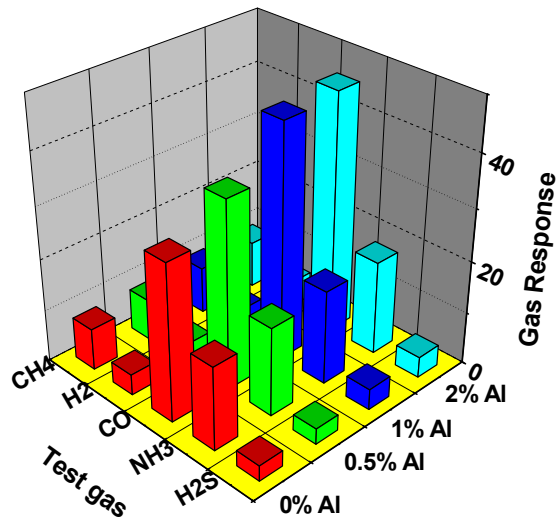
**Fig. 4 Effect of temperature on response of ZnO sensor for CO gas**

Fig. 4 shows the response of ZnO: Al thin film sensors as a function of temperature. It is seen that the response increases with temperature, reaches maximum at 250°C and further decreases. Thus, in the present case the optimum operating temperature for ZnO films is 250°C at which sensor response attained its peak value. This behavior can be explained as follows. At low operation temperatures, the low response can be expected because the gas molecules do not have enough thermal energy to react with the surface adsorbed oxygen species. With increase in temperature the thermal energy becomes high enough to overcome the potential barrier, and a significant increase in electron concentration was resulted from the sensing reaction. At higher temperatures the sensor response is restricted by the speed of diffusion of gas molecules. At some intermediate temperature, the speed values of the two processes become equal, and at that point the sensor response reaches its maximum [19, 20].

The ability of a sensor to respond to a certain gas in presence of other gases is known as selectivity. Here, the selectivity measured in terms of selectivity coefficient of a target gas to another gas is defined as  $K = S_A/S_B$ , where  $S_A$  and  $S_B$  are the responses of a sensor to a target gas and an interference gas, respectively. To check the selectivity of the sensor, it was exposed to various gases like H<sub>2</sub>S, NH<sub>3</sub>, CO, H<sub>2</sub> and NO<sub>2</sub>.

Fig. 5 shows the histogram of gas response of Al-doped thin films for different gases at a fixed concentration of 100 ppm. All the measurements were carried out at 250°C. The histogram revealed that the pure ZnO sensor offered response to H<sub>2</sub>S (3), NH<sub>3</sub> (16), CO (30), H<sub>2</sub> (4) and NO<sub>2</sub> (8). The ZnO film showed more selectivity for CO over other gases. The selectivity coefficient for CO over other gases has the values 10, 1.87, 7.5 and 3.75 against H<sub>2</sub>S, NH<sub>3</sub>, H<sub>2</sub> and NO<sub>2</sub>, respectively. This may be due to the different gases have different energies for reaction to occur on the surface of ZnO thin film [19].

When referred to the effect of Al-doping, it is observed that the sensor response increases with Al-doping concentration up to 1wt% and tends towards saturation for higher doping concentration. It is important to note that n-type semiconductor material such as ZnO have few oxygen adsorption sites available due to development of potential barriers on the particle surface. Consequently, incorporation of species which have comparatively higher number of adsorption sites with high fractional occupancy in the ZnO material can have significant impact on the sensor performance. The effect of doping can be explained as follows. Al-doping can have several effects on the properties important to gas sensing applications including inhibiting ZnO grain growth, creation of new donor levels, and modifying the gas-



**Fig. 5 Response of ZnO: Al sensor for various gases (Temperature 250°C)**

surface interactions [21]. From SEM studies it is observed that Al-doping increases the porosity of the film which increases the gas-surface interactions. Another important role of Al-doping is that substitution of  $Zn^{2+}$  by  $Al^{3+}$  acts as donor impurity thereby increasing the electron concentration. This results in decrease in electron Debye length thereby modifying the gas-surface interactions. The overall effect is enhancement in the sensing performance.

The gas sensing mechanism can be explained in terms of conductance modulation by adsorption of atmospheric oxygen on the surface and subsequent reaction of adsorbed oxygen with target gas. The atmospheric oxygen molecules are adsorbed on the surface of sensor. These molecules take electrons from the conduction band of n-type ZnO to be adsorbed as  $O_{2,ads}^-$  and  $O_{ads}^-$  leading to the formation of electron depleted region near the surface of ZnO particle. The form of the adsorbed oxygen (either molecule or atom) depends on the temperature of the sensor, where  $O_{2,ads}^-$  species have been observed at lower temperatures (below 175°C) and  $O_{ads}^-$  species have been observed at higher temperatures (above 175°C). Due to the formation of depletion region the material show high resistance state in air ambient. On exposure, the CO gas molecules react with negatively charged oxygen adsorbates and the trapped electrons are given back to conduction band of ZnO. The energy released during this process would be sufficient for electrons to jump up into the conduction band of zinc oxide, causing an increase in the conductivity of the sensor [20]. So the steady state value of the resistance depends on the concentration of the CO gas. The overall reactions are as follows:



And



Incorporation of aluminum in zinc oxide has a significant impact on the sensor performance. The  $\text{Al}^{3+}$  ions act as donor impurity thereby increasing the electron concentration. This results in decrease in electron Debye length, increases the oxygen adsorption sites and subsequently modifies the gas-surface interactions. The overall effect is enhancement in the sensing performance.

The response of the sensor as a function of time under the exposure to CO gas at 100 ppm concentration was studied (Fig. 6).

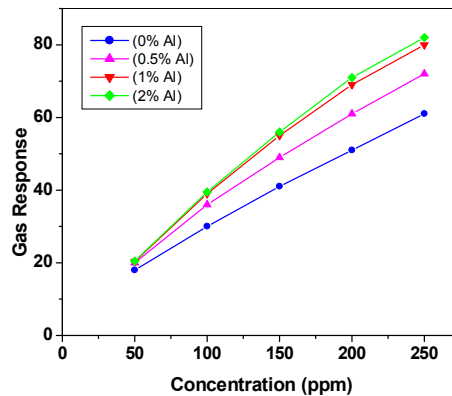


**Fig. 6 Response of ZnO: Al sensor for various concentrations of CO gas**

The conductivity increased rapidly by exposing the sensor to CO gas and recovered towards original value after introducing clean air. This demonstrates a high potential for nanostructured metal oxide sensors with superior sensitivity. The response and recovery times of the sensor were calculated and found to be of the order of 25 and 80 seconds, respectively. The variation of sensitivity with CO gas concentration showed that sensitivity increases almost linearly with the gas concentration up to 200 ppm and deviates afterwards (Fig. 7).

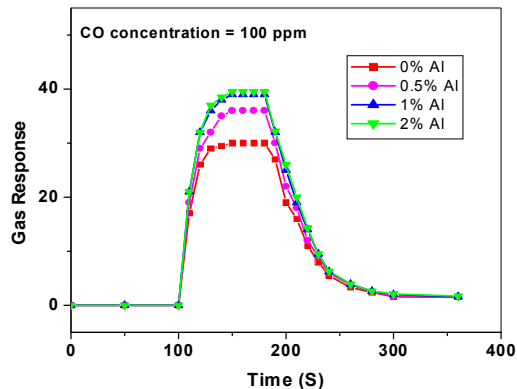


**Fig. 7 Speed response of ZnO: Al sensor**

At lower gas concentrations a monolayer of gas molecules would be formed on the surface of the sensor which interact more actively giving linear response. At higher gas concentrations, the multilayers of the gas molecules would result into deviation from linearity [22].

#### 4. CONCLUSION

In summary, Al-doped ZnO thin films were prepared using sol-gel spin coating technique. The XRD studies show synthesis of phase pure ZnO thin films with hexagonal wurtzite structure. The lattice parameters are  $a=3.2568\text{\AA}$  and  $c=5.2108\text{\AA}$  and decreases with Al-doping concentration. SEM studies show that with Al-doping the growth of the films takes place with porous structure embedded with nanogranules overgrown on the folded structure. Transmission electron microscopy also confirms the nanocrystalline nature of the samples. Gas sensing properties of the Al-doped ZnO thin films were systematically investigated and compared with those of the pure ZnO thin films. Obtained results showed that the Al-doped sensor has a good selectivity to CO with higher responses compared with the undoped sensor. The optimum operating temperature is found to be  $250^{\circ}\text{C}$ . The enhanced sensor response is due to small crystallite size, modifications in the electron Debye length and modifying the gas-surface interactions. The sensing mechanism is dominated by the generation of new trapped centers and defects introduced into ZnO lattice after Al-doping. This work also suggests that the Al-dopant can be a promising substitute for the noble metal additives to fabricate chemical sensors with a much lower cost.

#### ACKNOWLEDGEMENTS

The authors are also thankful to the Director, NEHU, Shilong, India for providing the TEM facility.

#### REFERENCES

- [1] Lupan, O.; Chai, G.; Chow, L.; *Microelectronic Engineering*, 2008, 85, 2220. DOI: 10.1016/j.mee.2008.06.021
- [2] Sucheai, M.; Christoulakis, S.; Moschovis, K.; Katsarakis, N.; Kiriakidis, G.; *Thin Solid Film* 2006, 515, 551. DOI: 10.1016/j.tsf.2005.12.295
- [3] Tamaekong, N.; Liewhiran, C.; Wistsoraat, A.; Phanichphant, S.; *Sensors*, 2010, 10, 7863. DOI: 10.3390/s100807863
- [4] Shinde, S. D.; Patil, G. E.; Kajale, D. D.; Gaikwad, V. B.; Jain, G. H.; *J. Alloys and Compounds*, 2012, 528, 109. DOI: 10.1016/j.jallcom.2012.03.020
- [5] Pawar, R.C.; Shaikh, J.S.; Suryavanshi, S.S.; Patil, P.S.; *Current Applied Physics*, 2012, 12, 778. DOI: 10.1016/j.cap.2011.11.005
- [6] Cao, Y.; Hu, X.; Wang, D.; Sun, Y.; Sun, P.; Zheng, J.; Ma, J.; Lu, G.; *Materials Letters*, 2012, 69, 45. DOI: 10.1016/j.matlet.2011.11.037
- [7] Seo, J.K.; Ko, K.; Cho, H. J. Choi, W.S.; Park, M.; Seo, K.; Park, Y.; Lim, D.G.; *Trans. Electr. Electron. Mater.*, 2010, 11(1), 29. DOI: 10.4313/TEEM.2010.11.1.029
- [8] Mondal, S.; Bhattacharyya, S.; Mitra, P.; *Pramana*, 2013, 80(2), 315. DOI: 10.1007/s12043-012-0463-6
- [9] Hu, P.; Han, N.; Zhang, D.; Ho, J.C.; Chen, Y.; *Sensors and Actuators B*, 2012, 169, 74. DOI: 10.1016/j.snb.2012.03.035
- [10] Patil, S.L.; Chougule, M.A.; Pawar, S.G.; Raut, B.T.; Sen, S.; Patil, V.B.; *J. Alloys and Compounds*, 2011, 509, 10055. DOI: 10.1016/j.jallcom.2011.08.030
- [11] Musat, V.; Rego, A.M.; Monteiro, R.; Fortunato, E.; *Thin Solid Films*, 2008, 516, 1512. DOI: 10.1016/j.tsf.2007.07.198
- [12] Vidap, R. V.; Mathe, V. L.; Shahane, G. S.; *J. Mater. Sci.: Mater. Electron.*, 2013, 24(9), 3170. DOI: 10.1007/s10854-013-1232-1

- 
- [13] Wang, X.; Wang, W.; Liu, Y.; *Sensors and Actuators B*, 2012, 168, 39. DOI: 10.1016/j.snb.2012.01.006
- [14] Li, X.; Chang, Y.; Long, Y.; *Materials Science and Engineering C*, 2012, 32, 817. DOI: 10.1016/j.msec.2012.01.032
- [15] Rout, C.S.; Raju, A.R.; Govindraj, A.; Rao, C.N.R.; *Solid State Communications*, 2006, 138, 136. DOI: 10.1016/j.ssc.2006.02.016
- [16] Kashyout, A. B.; Soliman, H. M. A.; Hassan, H. S.; Abousehly, A. M.; *J. Nanomaterials*, 2010, Article ID 341841, 8. DOI:10.1155/2010/341841
- [17] Lupan, O.; Shishiyanu, S.; Ursaki, V.; Khallaf, H.; Chow, L.; Shishiyanu, T.; Sontea, V.; Monaico, E.; Railean, S.; *Sol. Ener. Mater. Sol. Cell*, 2009, 93, 1417. DOI: 10.1016/j.solmat.2009.03.012
- [18] Vidap, R.; Shahane, G.; *Int. J. Adv. Engin. Tech.*, 2015, 8(5), 783. DOI: 10.7323/ijaet/v8\_iss5
- [19] Chougule, M.A.; Sen, S.; Patil, V.B.; *Ceramics International*, 2012, 38, 2685. DOI: 10.1016/j.ceram.2011.11.036
- [20] Patil, L.A.; Shinde, M.D.; Bari, A.R.; Deo, V.V.; *Sensors and Actuators B*, 2009, 143, 270. DOI: 10.1016/j.snb.2009.09.048
- [21] Miller, T.A.; Bakrania, S.D.; Perez, C.; Wooldridge, M.S. Nanostructured Tin Dioxide Materials for Gas Sensor Applications, In *Functional Nanomaterials* Geckeler, K.E.; Rosenberg, E. (Eds.); American Scientific Publishers, 2006, pp. 1-24.
- [22] Patil, S.L.; Chougule, M.A.; Sen, S.; Patil, V.B.; *Measurement*, 2012, 45, 243. DOI: 10.1016/j.measurement.2011.12.012